

OXFORD

Cerebral Cortex, March 2019;29: 1351–1368










doi: 10.1093/cercor/bhy322

Advance Access Publication Date: 7 January 2019




Original Article

ORIGINAL ARTICLE

I See Your Effort: Force-Related BOLD Effects in an Extended Action Execution–Observation Network Involving the Cerebellum

Letizia Casiraghi ^{1,2}, Adnan A.S. Alahmadi ^{3,4}, Anita Monteverdi ¹,
Fulvia Palesi ⁵, Gloria Castellazzi ^{4,6}, Giovanni Savini ^{2,7},
Karl Friston ⁸, Claudia A.M. Gandini Wheeler-Kingshott ^{1,4,9}
and Egidio D'Angelo ^{1,2}

¹Department of Brain and Behavioral Sciences, University of Pavia, 27100 Pavia, Italy, ²Brain Connectivity Center, IRCCS Mondino Foundation, 27100 Pavia, Italy, ³Diagnostic Radiography Technology Department, Faculty of Applied Medical Science, King Abdulaziz University (KAU), Jeddah 80200-21589, Saudi Arabia, ⁴NMR Research Unit, Queen Square Multiple Sclerosis (MS) Centre, Department of Neuroinflammation, Institute of Neurology, University College London (UCL), WC1N 3BG London, UK, ⁵Brain MRI 3T Center, Neuroradiology Unit, IRCCS Mondino Foundation, Pavia, PV, Italy, ⁶Department of Electrical, Computer and Biomedical Engineering, University of Pavia, 27100 Pavia, Italy, ⁷Department of Physics, University of Milan, 20133 Milan, Italy, ⁸Wellcome Trust Centre for Neuroimaging, Institute of Neurology, University College London (UCL), WC1N 3BG London, UK and ⁹Brain MRI 3T Mondino Research Center, IRCCS Mondino Foundation, 27100 Pavia, Italy

Address correspondence to Letizia Casiraghi. Email: letizia.casiraghi@gmail.com; Claudia A.M. Gandini Wheeler-Kingshott. Email: c.wheeler-kingshott@ucl.ac.uk; Egidio D'Angelo. Email: dangelo@unipv.it  orcid.org/0000-0002-2366-1835,  orcid.org/0000-0002-4832-1300,  orcid.org/0000-0002-6007-7187

Claudia A.M. Gandini Wheeler-Kingshott and Egidio D'Angelo contributed equally to this work.

Abstract

Action observation (AO) is crucial for motor planning, imitation learning, and social interaction, but it is not clear whether and how an action execution–observation network (AEON) processes the effort of others engaged in performing actions. In this functional magnetic resonance imaging (fMRI) study, we used a “squeeze ball” task involving different grip forces to investigate whether AEON activation showed similar patterns when executing the task or observing others performing it. Both in action execution, AE (subjects performed the visuomotor task) and action observation, AO (subjects watched a video of the task being performed by someone else), the fMRI signal was detected in cerebral and cerebellar regions. These responses showed various relationships with force mapping onto specific areas of the sensorimotor and cognitive systems. Conjunction analysis of AE and AO was repeated for the “0th” order and linear and nonlinear responses, and revealed multiple AEON nodes remapping the detection of actions, and also effort, of another person onto the observer’s own cerebrotocerebellar system. This result implies that the AEON exploits the cerebellum, which is known to process sensorimotor predictions and simulations, performing an internal assessment of forces and integrating information into high-level schemes, providing a crucial substrate for action imitation.

© The Author(s) 2019. Published by Oxford University Press.

This is an Open Access article distributed under the terms of the Creative Commons Attribution License (<http://creativecommons.org/licenses/by/4.0/>), which permits unrestricted reuse, distribution, and reproduction in any medium, provided the original work is properly cited.

Key words: action execution, action observation, cerebellum, functional magnetic resonance imaging, grip force

Introduction

Social behavior is based on understanding the actions of others and predicting appropriate reactions and subsequent interactions. In this context, perceiving the force applied to objects by others is crucial for understanding their intentions, for predicting the success of self-generated actions, and for dynamic movement control in interactions. However, there is still debate over the question of whether, when observing someone else performing an action, we mirror the actual movement dynamics or simply its goals (Calvo-Merino et al. 2006; Filimon et al. 2007; Thompson et al. 2007; Hamilton and Grafton 2008; Caspers et al. 2010; Cavallo et al. 2015; Koul et al. 2018). Understanding, through observation, the force involved in movements performed by others can prime the force imparted during subsequent action executions (AE) (Salama et al. 2011). The achievement of a better understanding of how force is represented in observation could facilitate and improve the clinical application of action observation (AO) in neurorehabilitation (Porro et al. 2007; Garrison et al. 2013; Buccino 2014). Although AE and observation have been studied using several techniques (Munzert et al. 2009; Sevdalis and Keller 2011; Vanderwert et al. 2013; Naish et al. 2014; Valchev et al. 2015), the neuronal processes involved in mirroring the motor effort of others have still not been fully explored.

The most renowned imitation learning hypothesis claims that “mirror neurons” are activated by observation of actions performed by others (Rizzolatti and Craighero 2004) and that the brain simulates the observed action by using the motor system as a forward model (Buccino et al. 2001; Miall 2003; Kilner et al. 2007; Ito 2008; Turella et al. 2009), recruiting hierarchically organized brain circuits (Kilner 2011; D’Angelo and Gandini Wheeler-Kingshott 2017). On a broader perspective, the brain has been proposed to include a “mirroring system” which can understand the intentions of others from observing movements (“body” reading) and a “mentalizing system” which can infer the intentions of others reconstructing hypothetical events (“mind” reading) (Van Overwalle and Baetens 2009; Van Overwalle, D’aes et al. 2015). In this context, even though magnetic resonance imaging (MRI) does not allow neuronal populations to be studied directly, functional MRI (fMRI), thanks to the blood-oxygenation-level-dependent (BOLD) effect (Kim and Ogawa 2012), can be used to study neuronal activation during both execution and observation of actions. fMRI studies (Buccino et al. 2001; Caspers et al. 2010; Caligiore et al. 2013; McGregor and Gribble 2015) support the notion that, during observation of a complex motor task, the AE network (AEN) and the AO network (AON) combine to form an action execution–observation network (AEON), which provides the neural infrastructure for imitation learning. Although the “core AEON” structures are the premotor cortex and a limited number of parietal and temporal cortical areas (Grèzes and Decety 2001), it is now clear that the AEON also comprises the supplementary motor area and the inferior frontal gyrus, as well as large sections of the somatosensory and occipitotemporal cortices (Gatti et al. 2017). Furthermore, the cerebellum and basal ganglia have also been suggested to play a role in an extended circuit underlying action understanding (Caligiore et al. 2013), to the point that the cerebellum is now considered to play a role as an adaptive predictor in AO (Sokolov et al. 2017). This idea derives

from the general theory of cerebellar functioning, wherein the cerebellum is seen as a forward controller in behavioral schemes that concern the interaction of the body with the external world, instructing the cerebral cortex in a predictive manner (Cotterill 2001; Llinás 2009; Diedrichsen et al. 2010; Shadmehr and Mussa-Ivaldi 2012; Callan et al. 2013). Moreover, a growing body of evidence from both lesion and fMRI studies (Gazzola and Keysers 2009; Molenberghs et al. 2012; Christensen et al. 2014; Van Overwalle et al. 2014; Caligiore et al. 2017) suggests that the cerebellum plays a crucial role in action–perception coupling, coordinating the application of an appropriate force and its timing to generate movement, and thus operating in a forward mode (D’Angelo and Casali 2012; Avanzino et al. 2015; D’Angelo and Gandini Wheeler-Kingshott 2017). On these bases, it can be hypothesized that predicting how to move by observation entails processing of force and involves an extended AEON that includes the cerebellum together with a complex set of cortical areas.

In the present study, aiming to identify the network involved in force perception, we exploited a paradigm that recently showed how a complex set of linear and nonlinear BOLD responses are elicited in several brain regions, including the cerebellum, when varying the force applied to an object (Alahmadi, Pardini et al. 2015; Alahmadi, Samson et al. 2015; Alahmadi et al. 2017). We used this grip-force (GF) squeeze ball paradigm to assess whether: 1) the AON presents both linear and nonlinear BOLD-GF associations during observation of the squeeze ball task; 2) the AEN and the AON share a common neural substrate, corresponding to the extended AEON; and 3) regions identified as part of the AEON exhibit linear and nonlinear BOLD-GF associations. The results of this work indeed support the existence of force-related BOLD effects not only in AE but also in the extended AEON, which includes the cerebellum.

Materials and Methods

Subjects

A total of 14 right-handed healthy volunteers (9 females) were initially recruited for this study. However, 2 participants were excluded from further analysis: one who failed to follow the task instructions and another who presented head motion (translation in the z direction) >2 mm. The final sample thus comprised 12 subjects (7 females; mean age 26 ± 3.5 years). The handedness of each subject was evaluated using the Edinburgh handedness scaling questionnaire (Oldfield 1971); the mean laterality index was $82 (\pm 16)$. All participants had normal or corrected-to-normal vision. No subject had a history of neurological or psychiatric disease. All the participants received a detailed explanation of the experimental procedures before participating in the experiment. The local research and ethics committee approved the study and all participants gave their written informed consent.

MRI Scanner and Scanning Sequences

A 3 T Philips Achieva MR scanner (Philips Healthcare, Best, The Netherlands) with a 32-channel head coil was used to perform a 3D T1-weighted anatomical scan and 3 T2*-weighted echo-planar imaging (EPI) fMRI scans. The 3D T1-weighted sequence

acquisition parameters were as follows: 3D inversion-recovery prepared gradient-echo (fast field echo) sequence with inversion time (TI) 824 ms, echo time (TE)/repetition time (TR) 3.1/6.9 ms, flip angle 8° and voxel size 1 mm isotropic. The fMRI acquisition parameters were: TR/TE 2.5/35 ms, 2.7 mm thick slices with interslice gap of 0.3 mm positioned axial-oblique to include the cerebellum, $3 \times 3 \text{ mm}^2$ in-plane resolution, field of view $192 \times 192 \text{ mm}^2$, SENSE factor 2, flip angle 90° and 200 repeated volumes.

Experimental Design

All the participants completed 3 randomized event-related fMRI sessions (Fig. 1): AE, AO, and AO with visual cue (AOvc). In all cases, all the stimuli were projected onto the same white screen, which was kept in the same position throughout; short-sighted participants used nonmagnetic visual aid goggles. The 3 experimental sessions are described below.

Squeeze Ball Event-Related Paradigm

This paradigm, previously described elsewhere (Alahmadi, Pardini et al. 2015; Alahmadi, Samson et al. 2015; Alahmadi et al. 2017), consisted of a visuomotor event-related power grip task, in which the order and timing of trials and rest periods was optimized to introduce temporal jittering and randomization of the applied GF strength (see below). The task was performed using an MR-compatible sphygmomanometer inflation bulb (“squeeze ball”) connected to a computer suite (located outside the scanner room) running the fMRI paradigm presentation. Compression of the ball resulted in an air pressure measurement proportional to the force exerted, which was recorded at a sampling rate of 20 Hz. In all, 75 active trials were performed, divided equally into sets of 15 corresponding, respectively, to GF levels representing 20%, 30%, 40%, 50%, and 60% of the subject’s maximum voluntary contraction (MVC). MVC had previously been measured in each subject using the same force device (i.e., by asking the subject to continuously squeeze the power ball) and this value was used to set the GF target for each trial.

Trials were performed in a counterbalanced and randomized order as obtained using the OptSeq optimization software (<https://surfer.nmr.mgh.harvard.edu/optseq/>). The rest time between squeezing trials—this lasted between a minimum of 2 s and a maximum of 12 s, and was cued by a black crosshair located at the center of the screen—was also randomized to introduce temporal jittering between the task and data

acquisition. Rest time accounted for 55% of the whole fMRI session (500 s). The visual cue used in the trials was a black static horizontal bar (presented for 3 s), which indicated the target GF level to reach. This cue was projected onto an MR-compatible white screen and shown together with an interactive colored bar, indicating the actual force level reached and thus providing real-time feedback to the subject about his/her own performance. The GF task was performed with the right (dominant) hand during the AE session.

A female actor was also filmed while performing the task in the control room of the scanner suite. The resulting video showed her whole right hand and forearm, filmed against a plain colored background, with the palm facing up. While recording the task, the computer also recorded the visual feedback she received (i.e., the visual cue bar), which was used to create a further video (in which the cue bar was superimposed on the forearm and hand) to be used in the AOvc session. Premiere Pro CS5 (Adobe System Software, CA, USA) was used for video editing.

AO (AO and AOvc) Behavioral Sessions

Before and after the fMRI sessions, subjects underwent behavioral sessions during which they were asked to watch the AO and AOvc videos (the order of presentation of the videos was randomized among subjects) and to verbally report their own perception of the GF, that is, 20%, 30%, 40%, 50%, or 60% of the MVC of the actor’s hand shown squeezing the ball in the video (perceived GF). These sessions served to test their recognition of the GFs observed, to saturate any learning effect before the actual fMRI experiment, and to test possible differences in learning effects between the pre- and post-MRI behavioral sessions. The purpose of running 2 AO behavioral sessions, AO and AOvc, was to assess whether GFs can be appreciated from subtle (and natural) cues alone—as in the AO condition (e.g., changes in the color of the hand with increasing effort and accompanying tendon contraction)—or whether subjects also need to see symbolic visual feedback, as in the AOvc condition. Performance accuracy was assessed for each of the 5 GF levels by calculating the number of correct answers and the mean difference between the perceived GF (pGF) and the GF actually applied by the actor during the video recording (aGF).

AE Training Session

After the AO behavioral sessions, just before the fMRI one, subjects were trained using a 2-min paradigm having a design

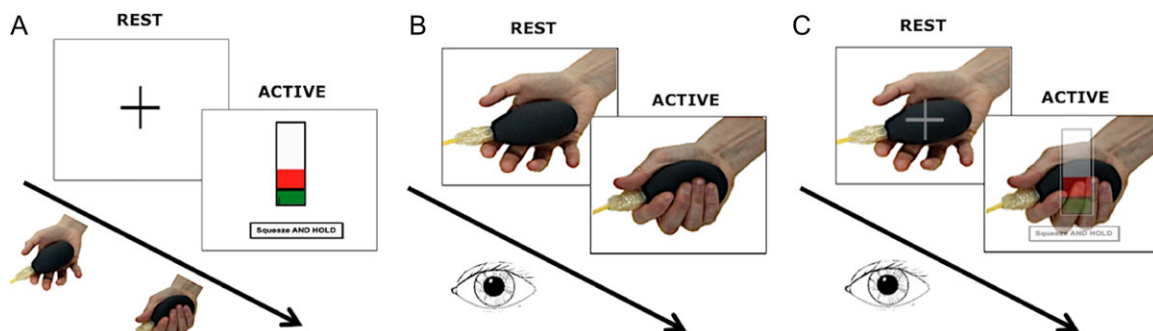


Figure 1. Experimental paradigm. The figure shows a pictorial representation of the 3 conditions that were used in the behavioral and fMRI sessions: (A) action execution (AE), (B) action observation (AO), and (C) action observation with visual cue (AOvc). The stimuli are shown above the arrow whereas the activity of the subject is shown below the arrow. During fMRI, every session lasted 8:33 min and the trials were administered in a counterbalanced and randomized order. The active trials (each lasting 3 s) were repeated 75 times and were divided equally between the 5 grip forces. A rest time of 2–12 s was allowed between active trials.

similar to the above-described event-related one, with GF levels ranging from 10% to 70% of their MVC. The training session involved practising the task outside the scanner bore.

AE Session

Subjects performed the AE task following the visual instructions described above. Their feedback was recorded at a sampling rate of 20 Hz during the task. The data collected served to include subject-specific performance in the statistical analysis.

AO Session

Subjects observed the video showing the right hand of the actor performing the squeeze ball task. They were asked to keep their gaze at the center of the projection screen indicated by a cross during rest periods, to relax, not to touch the squeeze ball, and to think about nothing throughout this fMRI recording session (as opposed to trying to guess the force or the next action).

AOvc Session

The subjects received the same instructions as in the AO session. The only difference, compared with the AO condition, concerned the stimuli: the video again showed the actor's right hand performing the squeeze ball task, but this time the image was overlaid with a translucent representation of the visual feedback that the actor had received during the recording of the video (thus an indication of her performance). This session was originally included as part of the behavioral study as it was unclear whether force perception demands some kind of visual feedback on the performance, such as that provided by the real-time bar (symbolic guided action observation). However, since the AO condition alone was found to be sufficient to disclose perception of force-related effects, the AOvc data were not considered further for the purposes of this study.

Data Analysis

Behavioral Data Analysis

The group mean accuracy of the subjects' perceptions (pGF) was calculated overall by measuring all correct responses as a percentage of all perceived forces (at 20%, 30%, 40%, 50%, and 60% of MVC of the hand squeezing the ball in the video), and also separately for each of the following sessions: AO before MRI, AOvc before MRI, AO after MRI, and AOvc after MRI. A number of statistical tests were performed. First, we used paired sample *t*-tests to assess possible significant differences between ratings in the AO versus the AOvc sessions; that is, considering the mean accuracy of pGF in the 2 conditions (considering "AO before MRI" vs. "AOvc before MRI" and then "AO after MRI" vs. "AOvc after MRI"). Second, a repeated measures ANOVA with Bonferroni correction was implemented to investigate learning effects, that is, testing for different performances within the AO and the AOvc sessions ("AO before MRI" vs. "AO after MRI" and then "AOvc before MRI" vs. "AOvc after MRI"). A statistical threshold of $P < 0.001$ was considered significant. Finally, to characterize the challenging nature of the AO task, we assessed the correlation between the actor's actual performance (i.e., the GF applied by the actor performing the task and recorded while filming) and the subjects' perceptions of that GF (i.e., the pGF, as reported by each subject during the "AO before MRI" behavioral session), using the correlation

coefficient (*r*) and the significance level (*P*-value). The statistical analysis was performed using the Statistical Package for the Social Sciences (SPSS) software (version 21.0).

fMRI Data Analysis

Whole Brain

Image analysis was performed with SPM12 (www.fil.ion.ucl.ac.uk/spm), implemented in Matlab15b (Mathworks, Sheborn, MA), using conventional preprocessing steps: slice timing, realignment, coregistration, estimation of (nonlinear spatial) normalization parameters between the 3D T1-weighted volume and the standard SPM12 template, application of the normalization parameters to the fMRI EPI volumes, and smoothing with an 8 mm isotropic full-width half maximum (FWHM) Gaussian kernel. The GF trials were modeled as delta functions (Friston et al. 1998) with parametric modulation according to GF. A general linear model (GLM) including polynomial expansions up to the fourth order was applied following the procedures described by Alahmadi et al. (Alahmadi, Pardini et al. 2015; Alahmadi, Samson et al. 2015). As discussed in previous work, the polynomial expansion allows nonlinear relationships to be characterized in an unbiased way, by modeling a mixture of linear and nonlinear responses in a parsimonious fashion. Interpretation of the nonlinear order lends itself to hierarchical testing (e.g., second-order effects are interesting only after removing first-order effects) (Büchel et al. 1998) and neurophysiological studies have reported different response profiles that have distinct nonlinear forms (Evarts 1968; Smith et al. 1975; Cheney and Fetz 1980; Riehle et al. 1994). Moreover, polynomial expansions are the most common form of expansion (in the absence of boundary conditions) when estimating neurometric functions from imaging data (Ward and Frackowiak 2003; Kuhtz-Buschbeck et al. 2008).

In our setting, the 0th order represents the main effect of hand gripping (executed or observed) compared with the rest condition, irrespective of the level of GF applied. The first order represents any linear dependency on GF level (executed or observed), while nonlinear orders represent more complicated neurometric functions such as U-shaped (second order), sigmoid (third order) and quadratic (fourth order) functions. The parametric modulation of the stick functions—encoding grip trials—with the polynomial expansion of GF produces stimulus functions that can then be convolved with a canonical haemodynamic response function for subsequent standard GLM analyses (Friston et al. 1998).

At the first level of analysis (within subject), the realignment parameters were included in the GLM as regressors of no interest (Friston et al. 1996) and *t* statistics were used to test for the effects of each polynomial coefficient. The associated contrast images of each of the 5 polynomial coefficients were then entered into a second (between-subject) level analysis and tested with one-sample *t*-tests, following standard procedures. The same analysis pipeline was followed for the AE and AO sessions. In the AO session, the GF levels corresponded to those recorded from the actor's performance. A voxel-wise threshold of $P_u < 0.001$ (minimum extent 5 voxels, $P_u = P$ uncorrected for multiple comparisons) was used to define clusters. A threshold of $P < 0.05$ was applied to the spatial extent of clusters that survived multiple comparisons corrections. The anatomical designations of significant clusters were determined using the SPM Anatomy Toolbox (Version 2.2b). The same criteria were used for AE and AO sessions.

SUIT

The fMRI analysis pipeline, optimized for whole-brain analysis, can give suboptimal results in the cerebellum (Diedrichsen 2006). Therefore, to focus on the cerebellum, we used SUIT (spatially unbiased infratentorial template), a high-resolution atlas template of the human cerebellum and brainstem, which is part of the SPM12 software package (Diedrichsen et al. 2009). The following steps were performed: 1) Extraction of each subject's cerebellum and brainstem from their corresponding whole-brain 3D T1-weighted anatomical images; 2) Normalization of the anatomical images to the SUIT template using nonlinear deformations; 3) Re-slicing of the functional contrast images produced from the first-level analysis using the deformation produced from step 2) and masking out activation outside the region of interest (i.e., the cerebellum). The normalized cerebellum functional contrast images (of each polynomial order) from each subject were then smoothed with an 8 mm FWHM Gaussian kernel and submitted to a (between-subject) standard second-level random effects analysis, testing for increasingly higher-order nonlinear effects within the cerebellum with one-sample *t*-tests. Significant clusters were defined using a height threshold of $P_u < 0.001$ (and a minimum extent of 5 voxels). The anatomical designations of regionally specific effects were defined using a high-resolution probabilistic atlas defined within the SUIT template (Diedrichsen et al. 2009). The resulting statistical parametric maps (SPMs) were projected on to the flat map of the cerebellum provided with the SUIT template (Diedrichsen and Zotow 2015).

Conjunction

To identify, in terms of a parametric response to GF, the extended AEON, engaged both in AE and AO, we performed a simple conjunction analysis. This entailed testing for action observation effects at a corrected level of significance within a search volume defined by AE.

We first used the SPM, testing for 0th order effects in order to localize the combined effect of AE and AO independently of GF, that is, to identify regions that showed a conjunction of AE/AO effects, irrespective of parametric force effects. We then

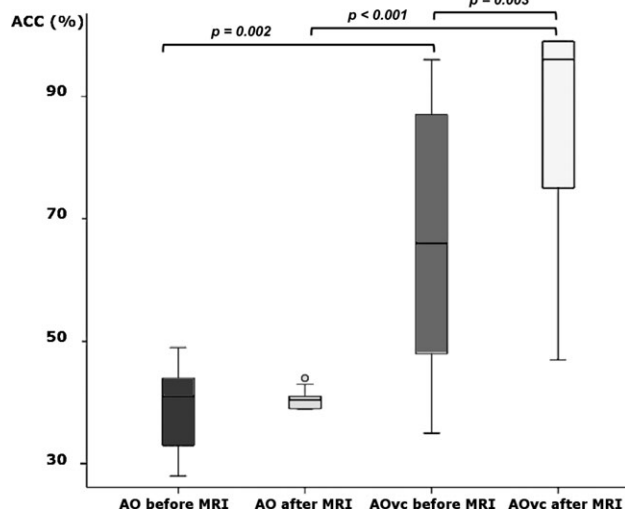


Figure 2. Group performance during action observation behavioral tasks. The box plot shows the relative accuracy (ACC) of force estimation in the different action observation (AO) and action observation with visual cue (AOvc) behavioral sessions (before and after the fMRI sessions). Significant differences between conditions are indicated (paired *t*-test).

identified regions that showed potential nonlinear responses to GF in both action observation and execution. In order to do so, we used a full factorial design and SPMs of the *F* statistic, testing for one or more significant polynomial coefficients in both execution and observation to obtain maps of the combined AE/AO force-related effect (FRE). Specifically, we used the SPMs of the *F* statistic, testing for a parametric effect of GF under AE (threshold $P_u < 0.0001$ for the whole brain analysis and $P_u < 0.001$ for the SUIT analysis) as a localizing contrast to define a search region within which to identify nonlinear effects under action observation (using the equivalent *F* contrast and a small volume correction to $P < 0.05$). Finally, we used the *F* statistic of the first-order effects to investigate the linear FRE and the *F* statistic of the higher-order effects to investigate the nonlinear FRE.

Results

BOLD fMRI signals were recorded from 12 healthy subjects during one visuomotor and 2 visual tasks for the purpose of comparing brain activation under AE and AO conditions, when different GF levels are applied to an object (in this case a squeeze ball).

AO Behavioral Responses

The behavioral performance, at group level, when watching the AO and AOvc videos, is shown in Fig. 2. The accuracy of the perceived grip force (pGF) significantly differed between AO and AOvc, both before ($P = 0.002$) and after ($P = 0.00008$) the MRI session. Within the AOvc condition, pGF accuracy was higher after MRI ($P = 0.003$), while no significant differences were found in the AO condition ($P = 0.955$). As expected, GF recognition was higher in AOvc than AO (mean accuracy \pm SD, 76 ± 22 and 39 ± 7 , respectively), although at the end of the experiment, some subjects reported that the bar indicating levels of force (the visual cue) had not influenced their behavioral responses during AOvc. AO data showed a positive correlation between aGF and pGF ($r^2 = 0.98$, $P = 0.005$) (Fig. 3), thus, confirming that the

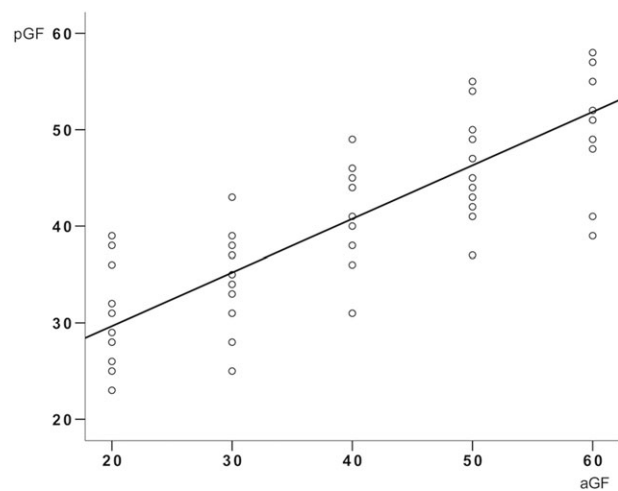


Figure 3. Relationship between applied and perceived grip force during the action observation behavioral task. The plot shows the relationship between grip force (GF) actually applied (aGF, i.e., GF presented on the video) and GF perceived (pGF, i.e., by the subjects watching the video) during the behavioral action observation (AO) task performed before and after fMRI recordings. The circles are individual subject responses and the line represents the group mean performance. A significant positive correlation was found between aGF and pGF ($R^2 = 0.98$, $P = 0.005$).

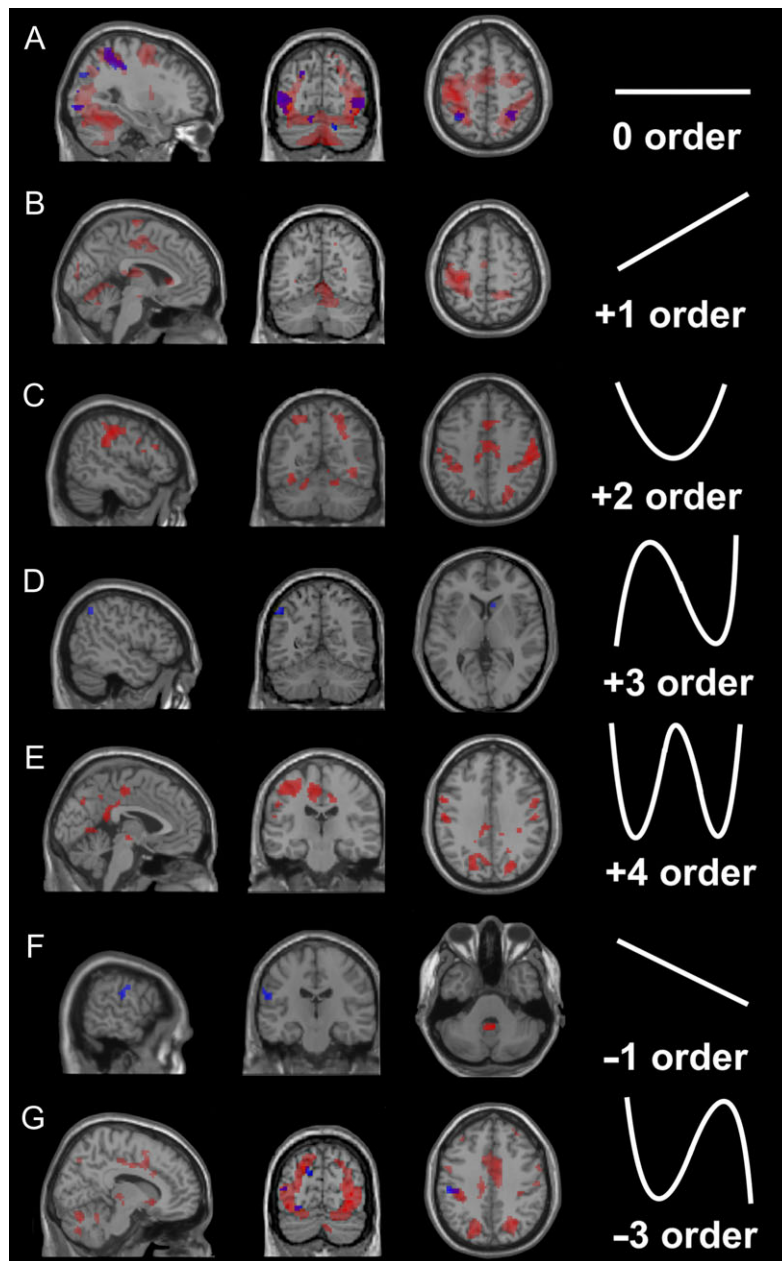


Figure 4. Whole-brain BOLD effects in action execution and observation. Brain maps at the group level corresponding to different orders of the BOLD-GF association in the action execution (AE, in red) and action observation (AO, in blue) conditions. The images show areas of activation at different orders. Note that both force-related and unrelated BOLD effects are found in the cerebral cortex and cerebellum. A threshold $P_u < 0.001$ ($k \geq 10$; $P_u = P$ uncorrected for multiple comparisons) was used for display purposes. The shape of the orthogonalised polynomial function that was fitted to the signals is shown for the (A) 0, (B) +1st, (C) +2nd, (D) +3rd, (E) +4th, (F) -1st, and (G) -3rd orders, to the right of the corresponding image showing significant clusters. In this and all the following figures, right is right and left is left.

subjects were able to infer the actor's movement in quantitative terms. Given that subjects correctly perceived the strength of the applied GF also when watching the AO video without the visual cue, subsequent analysis of fMRI data concerned only the AE and AO conditions.

Whole Brain—BOLD Effects

Regionally specific effects for 0th (main effect), linear (+1st, -1st) and nonlinear (+2nd, +3rd, +4th, -3rd) order responses were detected, using whole-brain analysis, on AE and AO. Full data with figures and tables detailing significant effects

(including coordinates, T values and cluster extents) are provided as supplementary material. AE activated many more regions than AO (Fig. 4), while both experimental conditions elicited regionally specific effects at 0th, -1st, and -3rd orders. Specifically, AO induced effects not only at the 0th order, but also at +3rd, 1st, and -3rd orders. These results reflect the presence of FRE during action observation.

Whole Brain Conjunction

AE and AO Main Effect (0th Order)

Several areas belonged to the extended AEON (in terms of a conjunction of zero order effects), and they included the

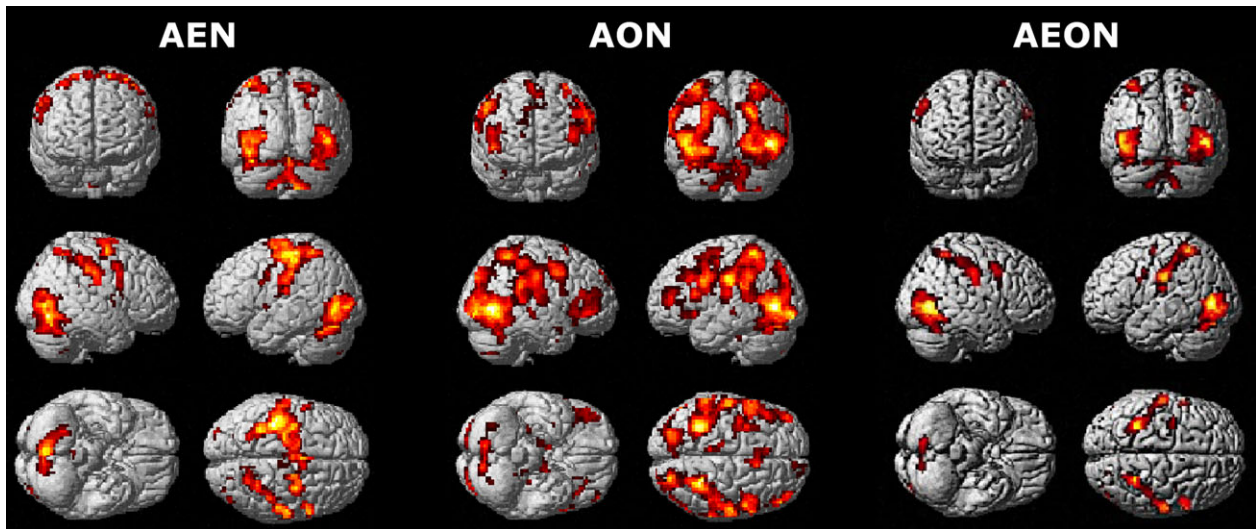


Figure 5. AEON: BOLD main effect. 3D whole-brain renderings of the main effects (0th order) in action execution (AEN), action observation (AON) and action execution-observation (AEON) networks. Note, in the AEON, the considerable overlap of effects in both the cerebral cortex and the cerebellum. Different thresholds were used for the 3 maps: $P_u < 0.0001$ ($k \geq 10$; $P_u = P$ uncorrected for multiple comparisons) was used for the AE condition; $P_u < 0.05$ ($k \geq 10$; $P_u = P$ uncorrected for multiple comparisons) was used for the AO condition; and $P < 0.05$ ($k \geq 10$), with a small volume correction applied to the AO map, was used to obtain the AEON.

Table 1 AEON: main effect (0th order)

Cluster	Peak				Anatomical region	BA/Loc (%)
	Ext	T	x	y		
1986	8.64	51	-67	-2	R Middle Temporal Gyrus*	hOc4la (51)
	8.23	-45	-73	2	L Middle Occipital Gyrus	hOc5 [V5/MT] (53)
	6.83	-42	-79	-5	L Inferior Occipital Gyrus	hOc4la (69)
534	6.6	-30	-49	55	L Inferior Parietal Lobule	7 PC (SPL) (31)
	6.12	-54	-22	28	L Postcentral Gyrus	PfT (IPL) (46)
439	6.3	30	-49	58	R Superior Parietal Lobule	7PC (SPL) (40)
	5.59	-34	-34	43	R Postcentral Gyrus	3a (25)/1 (35)
	4.7	57	-16	37	R Postcentral Gyrus	
76	5.32	60	8	19	R Precentral Gyrus	44 (50)
33	4.61	-57	5	31	L Precentral Gyrus	44 (10)
30	4.46	-36	-4	16	L Insular Lobe	
13	4.45	24	-70	37	R Superior Occipital Gyrus	
	3.26	21	-79	43	R Cuneus	7P (SPL) (9)
46	3.41	-33	-7	64	L Precentral Gyrus	
35	3.11	-9	-10	7	L Thalamus	Thal: Prefrontal (86)

The table reports all the action execution-observation network (AEON) regions that presented a main effect (0th order). The statistical threshold is set using $P < 0.05$ ($k \geq 10$) at the cluster level. Regions (*) survived a $P < 0.05$ correction for multiple comparisons at the peak level. The first cluster (ext = 1986) contains cerebellar activations (Crus 1 and lobules VI and VII). The last column reports the probability (expressed as a percentage) of these voxels being located in the respective Brodmann area (BA) or specific location (Loc) according to the cytoarchitectonic maps. ext = extension (number of voxels in a cluster); T = T-value at the voxel level. x, y, z are peak coordinates in MNI space (mm).

occipital and temporal lobes, inferior and superior parietal cortices, precentral and postcentral gyri, inferior frontal gyrus, insula, thalamus and cerebellum. The occipitotemporal cluster extended into the cerebellar lobules VI and VII and cerebellar Crus I (Fig. 5 and Table 1).

Force-Related Effects (Linear and Nonlinear Orders)

FREs (Fig. 6A and Table 2) were jointly expressed in several brain regions: supramarginal gyrus, calcarine gyrus, temporal gyrus, parietal lobe, insula, postcentral and precentral gyri, inferior frontal gyrus, middle cingulate cortex, posterior-medial and superior frontal cortices, rolandic operculum, lingual gyrus, basal

ganglia, and cerebellum. A limited number of brain regions, that is, the precentral and postcentral gyri (Fig. 6B), exhibited a linear FRE (+1st and -1st orders) in both AE and AO. The most prevalent joint FREs were nonlinear (+2nd, +3rd, +4th, -2nd, -3rd, -4th orders) and identified in the: supramarginal gyrus, angular gyrus, precentral and postcentral gyri, occipital lobe, inferior and middle temporal gyri, rolandic operculum, inferior and superior parietal cortices, inferior and middle frontal gyri, middle cingulate cortex, insula, thalamus and cerebellum (Fig. 6C).

SUIT—BOLD Effects

The AE condition detected more activated cerebellar regions than the AO one did (Fig. 7). In AE cerebellar specific effects

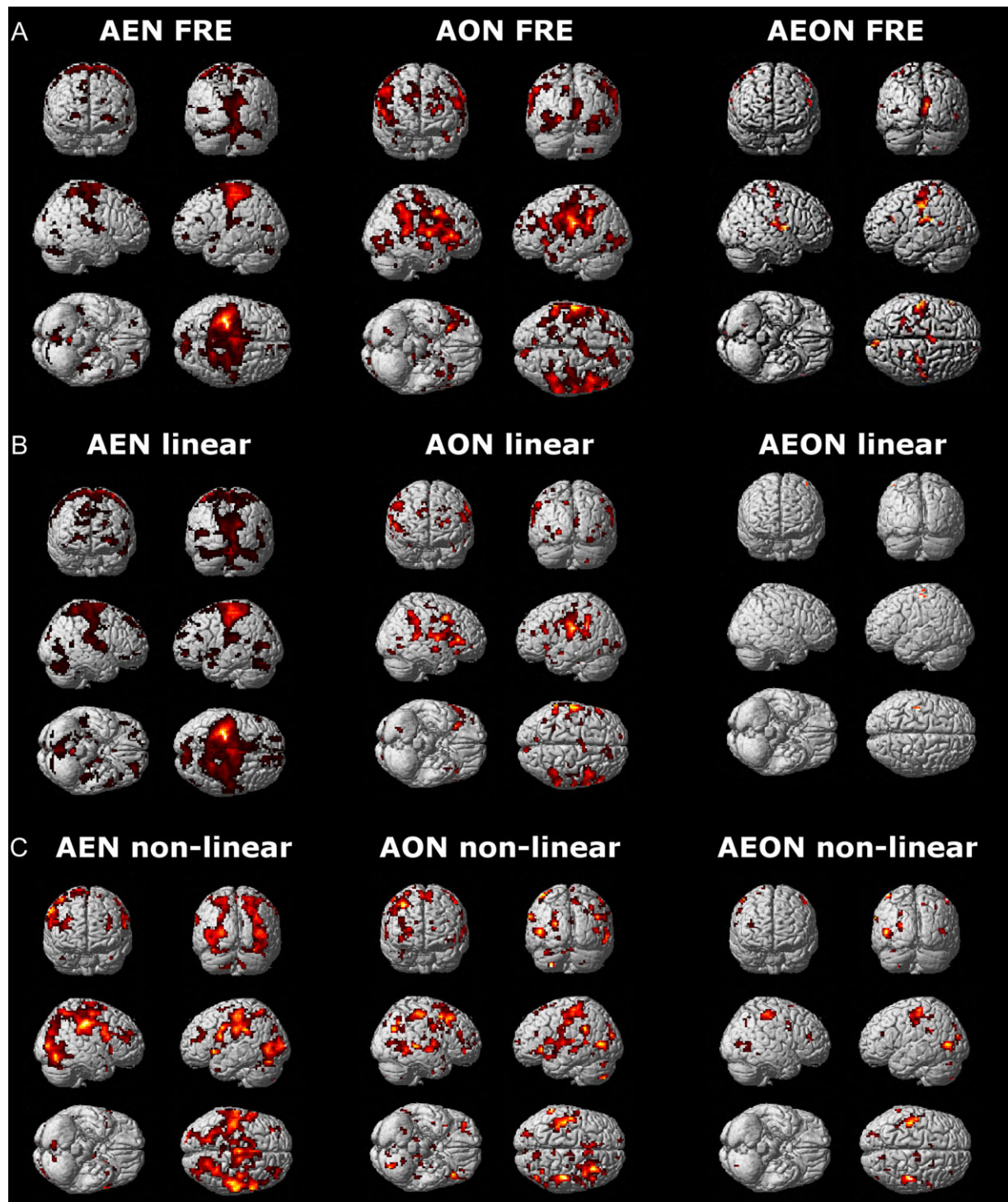


Figure 6. AEON: force-related BOLD effects. 3D whole-brain renderings of the force-related effects: (A) force-related effects (FRE), (B) linear force-related effects (linear FRE), and (C) nonlinear force-related effects (nonlinear FRE) in action execution (AEN), action observation (AON) and action execution–observation (AEON) networks. Note, in AEON, the prevalence of nonlinear associations in both the cerebral cortex and the cerebellum. Different thresholds were used for the 3 maps: $P_u < 0.0001$ ($k \geq 10$; $P_u = P$ uncorrected for multiple comparisons) was used for the action execution condition; $P_u < 0.05$ ($k \geq 10$; $P_u = P$ uncorrected for multiple comparisons) was used for the action observation condition; and $P < 0.05$ ($k \geq 10$), with a small volume correction applied to the AO map, was used to obtain the AEON.

were detected in lobule V and VIII (+1st order), lobule VI (0th and +4th orders), lobule VII (0th order), and Crus I (0th, +4th and –3rd orders). AO effects were observed in lobule VI (0th and –3rd orders), Crus I (0th order), and Crus II (+4th order).

SUIT—Conjunction

AE and AO Effect (0th Order)

Lobules VI and VII and Crus I and II were jointly involved in AE and AO (Fig. 8).

Table 2 AEON: force-related BOLD effects

Cluster ext ($k \geq 10$)	Peak				Anatomical region	BA/Loc (%)	
	T	x	y	z			
62	6.79	-3	20	-2	L Caudate Nucleus	33 (36)	
340	23.39	-54	-22	22	L Supramarginal Gyrus*	OP1 [SII] (53)	
	12.92	-45	-34	19	L Superior Temporal Gyrus*	PFcm (IPL) (56)	
	11.22	-48	-28	49	L Inferior Parietal Lobule*	2 (54)	
	10.11	-36	-16	10	L Insular Lobe*	Ig2 (56)	
	9.58	-57	-16	43	L Postcentral Gyrus*	1 (57)	
	8.5	-51	-22	40	L Inferior Parietal Lobule*	2 (46)	
	6.97	-51	-16	31	L Postcentral Gyrus*	3b (59)	
	5.2	-27	-22	70	L Precentral Gyrus		
	15	15.61	-57	26	22	L Inferior Frontal Gyrus (p. Triangularis)*	45 (64)
		9.16	-54	29	25	L Inferior Frontal Gyrus (p. Triangularis)*	45 (38)
226	15.41	9	2	52	R Posterior-Medial Frontal*		
	12.75	9	8	40	R Middle Cingulate Cortex*		
	8.38	0	-1	58	L Posterior-Medial Frontal*		
	7.62	-6	-10	55	L Posterior-Medial Frontal*		
	6.56	3	-19	49	R Posterior-Medial Frontal	4a (17)	
	3.97	0	-19	37	L Middle Cingulate Cortex		
	2.91	3	-10	34	R Middle Cingulate Cortex		
143	13.76	54	-7	10	R Rolandic Operculum*	OP4 [PV] (44)	
	13.39	60	2	10	R Rolandic Operculum*	44 (11)	
	11.65	66	-16	25	R SupraMarginal Gyrus*	PFop (IPL) (39)	
	7.8	51	-19	16	R Rolandic Operculum*	OP1 [SII] (64)	
	6.56	66	-19	13	R Superior Temporal Gyrus	TE 3 (31)	
	5.93	45	-28	16	R Superior Temporal Gyrus	OP1 [SII] (41)	
	3.57	57	-31	22	R Superior Temporal Gyrus	PFcm (IPL) (40)	
31	11.65	-3	-64	4	L Lingual Gyrus*	hOc1 [V1] (51)	
185	10.22	6	-91	16	R Cuneus*	hOc2 [V2] (74)	
	9.27	6	-94	10	R Cuneus*	hOc2 [V2] (73)	
	6.8	18	-73	4	R Calcarine Gyrus	hOc1 [V1] (75)	
	5.58	15	-79	1	R Lingual Gyrus	hOc1 [V1] (65)	
10	7.85	39	-19	43	R Precentral Gyrus	4p (54)	
24	7.14	15	-64	-26	R Cerebellum*	Lobule VI (Hem) (77)	
25	6.84	-12	-61	-17	L Cerebellum	Lobule VI (Hem) (94)	
13	6.65	21	-49	-23	R Cerebellum	Lobule VI (Hem) (77)	
38	6.42	-33	-46	67	L Superior Parietal Lobule	1 (7)	
	5.34	-24	-49	61	L Superior Parietal Lobule	5 L (SPL) (51)	
33	6.41	60	-13	43	R Postcentral Gyrus	1 (58)	
	3.01	51	-10	52	R Precentral Gyrus	4a (8)	
16	6.38	54	-67	-5	R Inferior Temporal Gyrus	hOc4la (68)	
	2.97	48	-73	4	R Middle Occipital Gyrus	hOc4la (72)	
97	6.25	30	-25	61	R Precentral Gyrus	4p (7)	
	5.84	48	-22	61	R Postcentral Gyrus	1 (22)	
	5.42	51	-25	58	R Postcentral Gyrus	1 (82)	
	4.56	21	-25	73	R Precentral Gyrus	4a (20)	
	12	6.21	-33	-13	22	L Insular Lobe	
15	6.16	-39	-76	7	L Middle Occipital Gyrus	hOc4la (26)	
10	5.82	15	41	1	R Anterior Cingulate Cortex		
23	4.8	21	-49	61	R Superior Parietal Lobule	5 L (SPL) (50)	
	4.66	27	-52	67	R Superior Parietal Lobule	7PC (SPL) (81)	
25	4.04	-15	-37	70	L Postcentral Gyrus	4a (26)	
	3.57	-18	-40	76	L Postcentral Gyrus	1 (16)	
13	3.66	15	-46	43	R Precuneus	5 Ci (SPL) (7)	
	3.19	12	-46	49	R Precuneus	5 Ci (SPL) (37)	

The table reports all the action execution-observation network (AEON) regions that presented a force-related effect (FRE). The statistical threshold is set using $P < 0.05$ ($k \geq 10$) at the cluster level. Regions (*) survived a $P < 0.05$ correction for multiple comparisons at the peak level. The last column reports the probability (expressed as a percentage) of these voxels being located in the respective Brodmann area (BA) or specific location (Loc) according to the cytoarchitectonic maps. ext=number of voxels in a cluster; T = T-value at the voxel level. x, y, z are the peak coordinates in MNI space (mm).

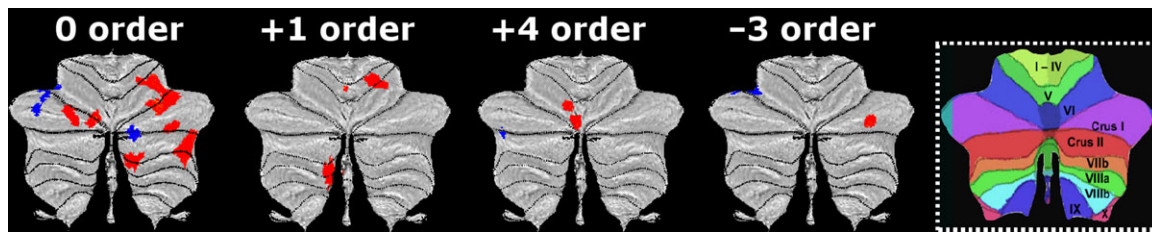


Figure 7. Cerebellar BOLD effects in action execution and observation. SUI flat maps at the group level corresponding to different orders of the BOLD–GF association in action execution (AE) and action observation (AO) conditions. Note the force-related and main (0th order) BOLD effects in different cerebellar areas. In the images, areas of activation at different orders of effect are shown for both AE (in red) and AO (in blue). A SUI flat map with labels of cerebellar lobules is shown in the bottom right corner. A threshold $P_u < 0.001$ ($k \geq 10$; $P_u = P$ uncorrected for multiple comparisons) was used for display purposes.

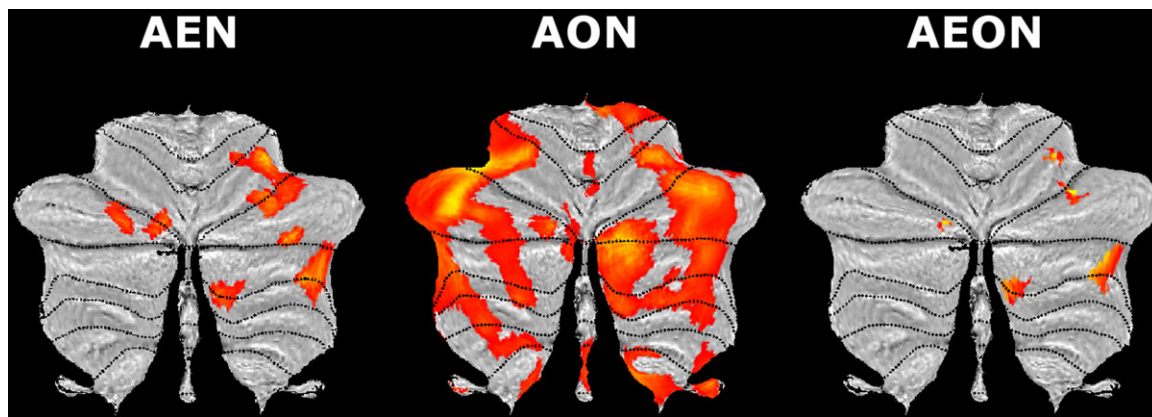


Figure 8. Cerebellar component of AEON: main BOLD effects. SUI flat maps of the main effects (0th order) in the cerebellar component of the action execution (AEN), action observation (AON) and action execution–observation (AEON) networks. Note, in AEON, the extended involvement of posterior and lateral areas of the cerebellum. Different thresholds were used for the 3 maps: $P_u < 0.001$ ($k \geq 10$; $P_u = P$ uncorrected for multiple comparisons) was used for the action execution condition; $P_u < 0.05$ ($k \geq 10$; $P_u = P$ uncorrected for multiple comparisons) was used for the action observation condition; and $P < 0.05$ ($k \geq 10$), with a small volume correction applied to the AON map, was used to obtain the AEON.

Force-Related Effects (Linear and Nonlinear Orders)

FREs were jointly identified in: Crus I and lobules V and VI (Fig. 9A). A cluster in lobule V presented a linear FRE (+1st and –1st orders) while a nonlinear FRE (+2nd, +3rd +4th, –2nd, –3rd, –4th orders) was found in 2 clusters in lobule VI and IX (Fig. 9B and C, respectively).

Discussion

In this study, we report for the first time the existence of force-related BOLD effects in an extended AEON involving cerebral and cerebellar regions that are both motor and associative in nature. These regions not only respond to observed and executed actions, but also share patterns of linear and nonlinear BOLD responses to parametric variations in GF. Linear BOLD–GF associations occurred in motor regions, while nonlinear BOLD–GF associations were found in regions specific to somatosensory state estimation, motor simulation and cognitive control. The cerebellum was found to be a key structure within the AEON, showing regional-specific correlations with force. These effects support the concept that the AEON extends to the cerebellum and to a set of cortical regions that are critical for imitation learning. The results are discussed and integrated with our current understanding of brain function in terms of the intrinsic functional connectivity of 7 fundamental networks (visual, somatomotor, ventral and dorsal attention, frontoparietal, limbic and default networks) (Yeo et al. 2011).

Behavioral Performance and Learning Effects

The subjects were found to be able to evaluate visually the efforts of others. There are 3 considerations indicating that this ability was independent of learning during the test (Weigelt et al. 2008). First, in order to saturate learning, all the subjects underwent AO training before the fMRI experimental sessions; this training is known to facilitate motor learning (Stefan et al. 2005; Salama et al. 2011) and increase force production by optimizing motor neuron recruitment (Porro et al. 2007). Second, the order of presentation of the AE, AO, AOvc sessions was randomized, thus limiting a potential variability in attentional load (e.g., induced by fatigue). Third, the accuracy in force detection was higher in AOvc than in the AO sessions. Therefore, independently of subject performance, the visual cue has a facilitator effect with respect to naturalistic stimulation (i.e., actual movement and changes in body parts during action), but the latter is nonetheless sufficient to perceive the intensity of another's movements.

It should be noted that in the AOvc condition we detected a learning effect, implying a facilitation of force recognition along trials. Moreover, we detected a higher variability of performance between participants in the AOvc compared with the AO condition; this might be due to attention being focused either on the visual cue or on the hand itself. However, the debriefing at the end of the experiment indicated that several participants had ignored the bar. For these reasons, we did not further consider the AOvc condition in our analysis.

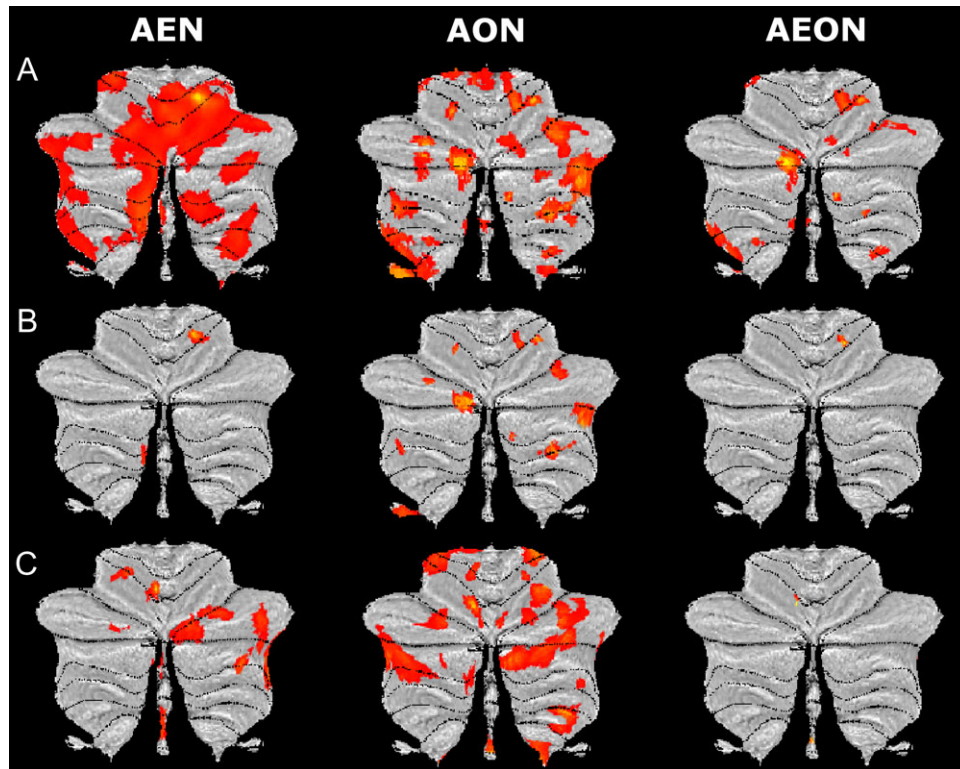


Figure 9. Cerebellar component of AEON: force-related BOLD effects. SUI flat maps of the (A) force-related effects (FRE), (B) linear force-related effects (linear FRE), and (C) nonlinear force-related effects (nonlinear FRE) in the cerebellar component of the action execution (AEN), action observation (AON) and action execution-observation (AEON) networks. Note, in AEON, the distribution of force-related BOLD effects over several cerebellar areas in the anterior and posterior cerebellum. Different thresholds were used for the 3 maps: $P_u < 0.001$ ($k \geq 10$; $P_u = P$ uncorrected for multiple comparisons) was used for the action execution condition; $P_u < 0.05$ ($k \geq 10$; $P_u = P$ uncorrected for multiple comparisons) was used for the action observation condition; and $P < 0.05$ ($k \geq 10$), with a small volume correction applied to the AON map, was used to obtain the AEON.

BOLD Effects Elicited by AE and AO

The BOLD effects elicited by AE occurred mostly in areas directly involved in motor planning, execution, and control (Alahmadi, Samson et al. 2015) (for a detailed description see Table 3). The main effect of AE was observed in premotor and sensorimotor cortices as well as in parietal, occipital and cerebellar cortices devoted to global sensorimotor processing (Neely et al. 2013) and included in visual, dorsal attention and somatomotor networks, while a linear activation with force was found in primary motor cortex and anterior cerebellum, that actually do encode force (Keisker et al. 2009) and belong to the somatomotor network. Nonlinear relationships with GF were found in parietal, frontal, cingulate and insular cortices, and in thalamus, basal ganglia and cerebellum, which form large-scale loops involved in the control of fine precision grip forces and motor learning (Graybiel 1998; Ehrsson et al. 2001; Kuhtz-Buschbeck et al. 2001). These loops could be linked with visual, ventral and dorsal attention, frontoparietal, somatomotor and default networks. Minor differences with previous squeeze ball studies (Alahmadi, Samson et al. 2015) could be related to the higher complexity of the present paradigm (which included behavioral training sessions and 3 different tasks).

The BOLD effects elicited by AO were recorded in an extended and distinctive set of occipital, parietal and frontal regions involved in motor but also sensory and cognitive processing (for a detailed description see Table 3). The main effect of AO was observed in the occipital and parietal regions related to motion perception and attention (Becker-Bense et al. 2012;

Thompson and Parasuraman 2012) that are considered to be part of the visual network and the ventral and dorsal attention networks. Linear responses with respect to GF occurred mainly in the postcentral gyrus, involved in processing proprioceptive and tactile representations of the manipulated object (Ebisch et al. 2008) and included in the somatomotor network. Nonlinear responses with respect to GF occurred in occipital and temporal cortices and inferior parietal lobule, involved in object recognition (Reed et al. 2004), inhibition of movement (Menon et al. 2001), spatial focusing of attention (Ptak 2012), and intention understanding (Koul et al. 2018). These functions are supported by the inclusion of activated regions in the visual, dorsal attention and default networks. These components, either main or FRES, probably provide the substrate for the interpretation and simulation of the actions of others (McGregor and Gribble 2015), while actual movement is inhibited.

The detection of specific nonlinear force-related BOLD effects in areas involved in AE or AO could imply complex task-related interplay of different neuronal populations (e.g., inhibitory and excitatory) within local networks. Understanding the biophysical basis of such nonlinearities will need realistic models and further investigation of neurovascular coupling under different conditions.

The Common Neural Substrate of AE and AO

The AEON, identified as the voxels shared by AEN and AON, was observed in cerebral cortex, thalamus, basal ganglia, and

Table 3 Summary of BOLD effects for AEN, AON, and AEON

Areas	AE			AO			AEON			Functions	References
	0 th	L	N	0 th	L	N	0 th	L	N		
Occipital											
Cuneus		#				§			°		Visual analysis of action/detection of biological motion/visual mental imagery of hand gesture/object recognition (Dupont et al. 1994; Hermsdörfer et al. 2001; Knauff et al. 2002; Rizzolatti and Craighero 2004; Wiggett and Downing 2011; Molenberghs et al. 2012; Romaguère et al. 2014; Ishibashi et al. 2016)
Fusiform OG			§	°		§				§	
Lingual OG			§								
Inferior OG	°			°					°		
Middle OG	°		§	°		§			°	§	
Superior OG			§	°		§			°	§	
Temporal											
Inferior TG			§							§	Visual motion processing/experience and observation of touch (Beer et al. 2002; Blakemore et al. 2005)
Middle TG				°	#	§				§	
Superior TG		#	§								
Hippocampus		#									
Parietal											
Postcentral PG	°	#	§	°	#		°	#	§	AE, AO and imitation/movement plan perception/proprioceptive representations/tactile simulation/spatial attention (Buccino et al. 2001; Grèzes and Decety 2001; Jovicich et al. 2001; Tanaka et al. 2001; Knauff et al. 2002; Gazzola and Keysers 2009; Shomstein 2012)	
Precuneus			§								
Inferior PG				°		§			°		§
Superior PG	°	#	§	°					°		§
Supramarginal G	°		§	°	#						§
Angular G											§
Frontal											
Precentral G	°	#	§	°		§	°	#	§	Mirror neurons/response inhibition/attention/inhibition of motor execution/motor goal/hand-object integration/motor planning/working memory (Cheng et al. 1995; Fagg and Arbib 1998; Shima and Tanji 1998; Brass et al. 2001; Grèzes and Decety 2001; Menon et al. 2001; Leung et al. 2002; Kasess et al. 2008; Morin and Grèzes 2008; Nakata et al. 2008; Caligiore et al. 2013)	
Inferior FG			§		#						§
Middle FG			§			§					§
Superior FG		#	§								§
Orbital FG		#									
Deep GM											
Thalamus	°	#	§						°	§	Modulation of movement, motivation and reward/modulation of motor preparation/force amplitude generation and prediction (Spraker et al. 2007; Wasson et al. 2010; Braadbaart et al. 2013; Caligiore et al. 2013)
Putamen			§								
Pallidum			§								
Caudate			§			§					
Amygdala		#				§					
Others											
Basal Forebrain		#	§								Maintenance of spatial attention during goal-directed actions/action style processing/sensorimotor integration/preparatory suppression of imitative responses (Luks and Simpson 2004; Cauda et al. 2012; Leech et al. 2012; Di Cesare et al. 2016; Campbell et al. 2018)
Brainstem						§					
ACC			§								
MCC	°	#	§							§	
PCC			§								
Insula			§	°	#		°			§	
Rolandic op			§							§	

(Continued)

Table 3 (Continued)

Areas	AE		AO		AEON		Functions	References
	0 th	L N	0 th	L N	0 th	L N		
Cerebellum								
Lobule V	#		°		#		Motor learning/observation of movements/control for movement	(Decety et al. 1997; Grèzes and Decety 2001; Spraker et al. 2007; Gazzola and Keysers 2009; Molenberghs et al. 2012; Stoodley et al. 2012; Buckner 2013; F KH et al. 2014; Weaver 2015)
Lobule VI	°	\$	°	\$	°	\$	execution/force amplitude generation and prediction/somatosensory state	
Lobule VII		\$					estimation/cognitive control	
Lobule VIII								
Crus 1	°	\$	°		°			
Crus 2				\$	°			
Lobule IX						\$		

The table reports all the action execution (AEN), action observation (AON), and action execution-observation (AEON) networks areas that showed main (0= 0th order) or force-related (L=linear, N = nonlinear) BOLD-GF relationships. The brain areas are listed and grouped by region: cerebellar lobes (occipital, temporal, parietal, and frontal), deep GM (gray matter), others and cerebellum. Three different symbols (°, #, \$) are used to indicate, respectively, the presence of main, linear or nonlinear effects in the corresponding area. Functions and references are reported for each group of regions. It should be noted that the thresholds used in the fMRI analysis differ depending on the condition (AE or AO) (see Materials and Methods). It has to be highlighted that the threshold problem is irrelevant for the conjunction analysis (AEON) columns because it refers to an independent analysis on overlapping. Bold type in the "areas" columns has been used to facilitate the location in the table of regions resulted from the conjunction analysis. G=Gyrus; OG=Occipital Gyrus; TG=Temporal Gyrus; PG=Parietal Gyrus; FG=Frontal Gyrus; op = operculum. ACC = Anterior Cingulate Cortex, MCC = Middle Cingulate Cortex, PCC = Posterior Cingulate Cortex.

cerebellum (Christensen et al. 2014) (for a detailed description see Table 3). The main effect of AEON was observed in occipital cortex, middle temporal gyrus, precentral and postcentral gyri, inferior and superior parietal lobules, insula, thalamus, and posterior cerebellum. These areas are involved in visual imagery of hand gestures, including visuospatial and motion processing (Hermsdörfer et al. 2001; Knauff et al. 2002), forward/inverse control for movement planning and execution, action style processing (Cauda et al. 2012), inhibition of motor execution to prevent imitative responses (Kilner 2011). These are, indeed, the fundamental ingredients of motor planning based on observation of actions (Caligiore et al. 2013). The activation of inferior and superior parietal lobules (which are part of the core mirror network) (Molenberghs et al. 2012) with occipital cortex, precentral and postcentral gyri and insula, suggest that AEON includes components from the visual, mirroring/somatomotor, ventral and dorsal attention networks.

The AEON areas showing FREs were also extensively distributed in occipital cortex, superior temporal gyri, inferior and superior parietal lobules, precentral and postcentral gyri, inferior frontal gyrus, medial frontal gyrus, precuneus, cingulate gyrus, caudate, thalamus, and cerebellum. These areas are involved in the experience and observation of touch (Blakemore et al. 2005), maintenance of spatial attention during goal-directed actions (Wasson et al. 2010; Cauda et al. 2012; Leech et al. 2012), sensorimotor integration, and force amplitude generation and prediction (Grèzes and Decety 2001; Blakemore et al. 2005). Moreover, the medial frontal gyrus is considered, with the temporoparietal junction, the "core network" of attribution of mental states (Schurz et al. 2014; Molenberghs et al. 2016) while the precuneus has been proposed to have a role in mental imagery to represent others' perspective (Cavanna and Trimble 2006). Therefore, FREs are particularly important in conferring the ability to detect the effort of others not just requiring the intervention of the mirroring/somatomotor, ventral and dorsal attention and frontoparietal networks but also of the mentalizing/default network.

Interestingly, activation in the AEON areas was mostly nonlinear, while linear relationships with GF were found only in a restricted part of the precentral and postcentral cortices (Gazzola and Keysers 2009) that are included in the mirroring/somatomotor network. Therefore, the AEON is engaged mainly in a nonlinear fashion during force processing.

Cerebellar Involvement in AEON

The cerebellum is known to operate as a generalized forward controller (D'Angelo and Casali 2012) that aids motor planning by predicting the sensory consequences of a motor act, such that a motor plan is coded in terms of an anticipatory sensory state (Blakemore, Goodbody et al. 1998; Blakemore, Wolpert et al. 1998; Callan et al. 2013). In the present context, the sensory state would be provided by AO, and motor predictions would be based on internal cerebellar representations of the system (body and muscle) state (Diedrichsen et al. 2010; Shadmehr and Mussa-Ivaldi 2012). Thus, the cerebellum is well geared for simulating movements after receiving information about the movement of others, in terms of the appropriate sequence (timing) and force (gain) (Yamazaki and Nagao 2012; Callan et al. 2013).

The cerebellum is strongly interconnected with the cerebral cortex through 7 fundamental resting-state networks (Yeo et al. 2011). In particular, Buckner et al. (2011) clearly identified in the cerebellum distinct mirroring and mentalizing networks (as

part of the larger somatomotor and default networks respectively) that were directly connected to homolog networks in the cerebral cortex. Confirming this network structure, Van Overwalle and colleagues reinterpreted their initial meta-analysis (Van Overwalle et al. 2014) in terms of this network structure and found strong evidence for it (Van Overwalle, Baetens et al. 2015). In addition, a meta-analytical connectivity analysis revealed a strong distinction between anterior mirroring and posterior mentalizing areas in the cerebellum linked to classic mirror and mentalizing areas in the cerebral cortex (Van Overwalle, D'aes et al. 2015). This was confirmed by functional connectivity studies relating mentalizing and executive control functioning to the cerebellum (Van Overwalle and Mariën 2016). Therefore, the cerebellum could also be involved in predicting the consequences and scope of other's actions by reconstructing hypothetical events (Buckner et al. 2011; Van Overwalle and Mariën 2016).

It should be noted that, in our study, cerebellar responses were embedded in a larger cluster that included occipitotemporal areas. The combined activation in the AEON in lobules VI and VII and Crus I and II could be considered part of the ventral and dorsal attention, frontoparietal, and mentalizing/default networks compounded by the mirroring/somatomotor network from specific FREs (Buckner et al. 2011). Indeed, the linear FRE in lobules V, part of the mirroring/somatomotor network, reveals the involvement of cerebellum in motor functions (Glickstein et al. 1994; Schmahmann 1996; Stoodley et al. 2012). The nonlinear effect in lobules VI and IX, part of both mirroring/somatomotor and mentalizing/default networks, would suggest the cerebellar involvement in the integration of motor processing and cognitive/emotional control (Stoodley and Schmahmann 2010).

Altogether, these effects confirm the cerebellar involvement in both mirroring and mentalizing networks. Moreover, these patterns of linear and nonlinear responses in the cerebellar components of the AEON are consistent with results showing that motor-generating areas respond linearly with GF, while associative and cognitive areas have a more complex relationship with GF. These response profiles may reflect distributed responses, mediated by connections that have been characterized structurally and physiologically in rodents, primates, and humans (Schmahmann and Pandya 1995; Kelly and Strick 2003; Ramnani 2006; Strick et al. 2009; Watson et al. 2014; Palesi et al. 2015, 2017).

High-Order Force–BOLD Relationships in the Cerebellum and Cerebral Cortex

While a monotonic relationship between BOLD response and GF levels was found in primary motor areas (M1 and anterior cerebellum)—and could be related to the increased neuronal recruitment with increasing GF (Cramer et al. 2002; Keisker et al. 2009)—nonlinearities were typically detected in areas implicated in multimodal integration and higher aspects of motor control (premotor, associative and sensory areas both in the cerebral cortex and the cerebellum), where a complex blend of signals converges to regulate motor output. It has been previously argued (Alahmadi, Samson et al. 2015) that second-order responses at intermediate force levels could be “metabolically optimal” and reflect more efficient processing in a motor regime requiring fewer corrective actions and less attention to sensory inputs. For example, nonlinearity may be due to fluctuation of attention levels modulating neural activity (Binkofski et al. 2002). However, it should be appreciated that it is difficult

to make detailed neurophysiological inferences based exclusively on fMRI signals. For example, nonlinearities (including nonlinear neuronal responses, nonlinear engagement of local inhibitory circuits, nonlinear mapping from neuronal activity to haemodynamic responses and finally, nonlinearities associated with the haemodynamic response function generating T2* signals) could arise at a number of different levels (Friston et al. 2000; Mechelli et al. 2001). The engagement of the underlying neuronal circuits, both in the cerebral cortex and the cerebellum, may benefit from further investigation using repetition-suppression fMRI paradigms (Kilner 2011; Barron et al. 2016) or multivoxel pattern analysis (Turella et al. 2009) in conjunction with animal recordings and large-scale model simulations (D'Angelo and Gandini Wheeler-Kingshott 2017).

Potential Limitations

Despite the coherent functional framework emerging from this investigation, the relatively small number of subjects may affect its statistical power in detecting active areas. Although previous studies used similar numbers of subjects, a larger sample may be beneficial to confirm our findings. However, it is important to note that significant results obtained using a small sample usually mean that the effect size is large (Flandin and Friston 2017). From a statistical point of view, the use of parametric models is an efficient way of accommodating nonlinear (neurometric) response functions within the established GLM framework (Friston 2012). However, given the concern that detection of active areas may have been reduced because of habituation due to multiple engagement in AO (Krekelberg et al. 2006), it would be useful to devise alternative paradigms in order to refine our AEON parametric characterization.

Conclusions

The extended AEON identified in this fMRI study engages large-scale brain networks capable of remapping the visual detection of the actions, and also effort, of others onto the observer's own motor system. These circuits, furnish not only understanding of other people's goals, that is, the “mirror” effect (Rizzolatti and Craighero 2004), but also the building blocks of executive control, impacting on various aspects of motor planning and programming, working memory, selective attention, and behavioral inhibition (Rizzolatti and Craighero 2004; Calvo-Merino et al. 2006; Filimon et al. 2007; Thompson et al. 2007; Hamilton and Grafton 2008; Caspers et al. 2010; Cavallo et al. 2015). The cerebrocerebellar loops, using the motor system as a forward model (Miall 2003; Kilner et al. 2007; Ito 2008; D'Angelo and Casali 2012; Callan et al. 2013), could play a crucial role in sensorimotor prediction and internal simulation of movement. It has been suggested that the insular and cingulate cortices, activated in parallel to the sensorimotor loops, allow exteroception to be integrated with interoception (Bodegård et al. 2001; Craig 2003; Pineda et al. 2009) and external observational cues to be transformed into internal sensorimotor plans. The identification of this extended AEON as a plausible substrate for imitation learning could facilitate and improve the clinical application of action observation in neurorehabilitation (Porro et al. 2007; Garrison et al. 2013; Buccino 2014).

Supplementary Material

Supplementary material is available at *Cerebral Cortex* online.

Funding

This work was performed at the Nuclear Magnetic Resonance (NMR) Research Unit (University College London (UCL), UK), which is funded by a program grant from the UK Multiple Sclerosis Society (892/08) and receives generous support from the Department of Health's National Institute for Health Research Biomedical Research Centres (BRC, Capital Project Number R&D03/10/RAG0449). C.G.W.K. receives support from International Spinal Research Trust (ISRT), Wings for Life (WfL), and Craig H Neilsen Foundation (CHNF) (the INSPIRED study), the UK Multiple Sclerosis Society (Grant 77) and H2020-EU.3.1 (634 541). Data analysis was performed at the Center for Health and Technology of the University of Pavia through the support of the Human Brain Project (HBP-720270 and 785907) to E.D. L.C. was supported by project HBP—Regione Lombardia (Grant Agreement 720270) and by Ministero della Salute (RC2015, 2016, 2017). F.P. is supported by the Italian Ministry of Health (5 per mille 2014). K.J.F. is funded by a Wellcome Trust Principal Research Fellowship (088 130/Z/09/Z). Further support comes from the Functional Imaging Laboratory (FIL, University College of London, UCL), and National Institute for Health Research (NIHR) Biomedical Research Centre (BRC) University College London Hospitals/University College London (UCLH/UCL) High Impact Initiative.

Notes

We would also like to acknowledge Sasha Ondobaka, Francesco Rigoli and James Kilner for useful discussions at the work beginning. *Conflict of Interest:* None declared.

References

- Alahmadi AA, Pardini M, Samson RS, D'Angelo E, Friston KJ, Toosy AT, Gandini Wheeler-Kingshott CA. 2015. Differential involvement of cortical and cerebellar areas using dominant and nondominant hands: an fMRI study. *Hum Brain Mapp.* 36:5079–5100.
- Alahmadi AA, Pardini M, Samson RS, Friston KJ, Toosy AT, D'Angelo E, Gandini Wheeler-Kingshott CA. 2017. Cerebellar lobules and dentate nuclei mirror cortical force-related-BOLD responses: beyond all (linear) expectations. *Hum Brain Mapp.* 38:2566–2579.
- Alahmadi AA, Samson RS, Gasston D, Pardini M, Friston KJ, D'Angelo E, Toosy AT, Wheeler-Kingshott CA. 2015. Complex motor task associated with non-linear BOLD responses in cerebro-cortical areas and cerebellum. *Brain Struct Funct.* 221:2443–2458.
- Avanzino L, Bove M, Pelosin E, Ogliastro C, Lagravinese G, Martino D. 2015. The cerebellum predicts the temporal consequences of observed motor acts. *PLoS One.* 10:e0116607.
- Barron HC, Garvert MM, Behrens TE. 2016. Repetition suppression: a means to index neural representations using BOLD? *Philos Trans R Soc Lond B Biol Sci.* 371:1–14.
- Becker-Bense S, Buchholz HG, zu Eulenburg P, Best C, Bartenstein P, Schreckenberger M, Dieterich M. 2012. Ventral and dorsal streams processing visual motion perception (FDG-PET study). *BMC Neurosci.* 13:81.
- Beer J, Blakemore C, Previc FH, Liotti M. 2002. Areas of the human brain activated by ambient visual motion, indicating three kinds of self-movement. *Exp Brain Res.* 143:78–88.
- Binkofski F, Fink GR, Geyer S, Buccino G, Gruber O, Shah NJ, Taylor JG, Seitz RJ, Zilles K, Freund HJ. 2002. Neural activity in human primary motor cortex areas 4a and 4p is modulated differentially by attention to action. *J Neurophysiol.* 88:514–519.
- Blakemore SJ, Bristow D, Bird G, Frith C, Ward J. 2005. Somatosensory activations during the observation of touch and a case of vision-touch synaesthesia. *Brain.* 128:1571–1583.
- Blakemore SJ, Goodbody SJ, Wolpert DM. 1998. Predicting the consequences of our own actions: the role of sensorimotor context estimation. *J Neurosci.* 18:7511–7518.
- Blakemore SJ, Wolpert DM, Frith CD. 1998. Central cancellation of self-produced tickle sensation. *Nat Neurosci.* 1:635–640.
- Bodegård A, Geyer S, Grefkes C, Zilles K, Roland PE. 2001. Hierarchical processing of tactile shape in the human brain. *Neuron.* 31:317–328.
- Braadbaart L, Williams JH, Waiter GD. 2013. Do mirror neuron areas mediate mu rhythm suppression during imitation and action observation? *Int J Psychophysiol.* 89:99–105.
- Brass M, Zysset S, von Cramon DY. 2001. The inhibition of imitative response tendencies. *Neuroimage.* 14:1416–1423.
- Buccino G. 2014. Action observation treatment: a novel tool in neurorehabilitation. *Philos Trans R Soc Lond B Biol Sci.* 369:20130185.
- Buccino G, Binkofski F, Fink GR, Fadiga L, Fogassi L, Gallese V, Seitz RJ, Zilles K, Rizzolatti G, Freund HJ. 2001. Action observation activates premotor and parietal areas in a somatotopic manner: an fMRI study. *Eur J Neurosci.* 13:400–404.
- Büchel C, Holmes AP, Rees G, Friston KJ. 1998. Characterizing stimulus-response functions using nonlinear regressors in parametric fMRI experiments. *Neuroimage.* 8:140–148.
- Buckner RL. 2013. The cerebellum and cognitive function: 25 years of insight from anatomy and neuroimaging. *Neuron.* 80:807–815.
- Buckner RL, Krienen FM, Castellanos A, Diaz JC, Yeo BT. 2011. The organization of the human cerebellum estimated by intrinsic functional connectivity. *J Neurophysiol.* 106:2322–2345.
- Caligiore D, Pezzulo G, Baldassarre G, Bostan AC, Strick PL, Doya K, Helmich RC, Dirx M, Houk J, Jörntell H, et al. 2017. Consensus paper: towards a systems-level view of cerebellar function: the interplay between cerebellum, basal ganglia, and cortex. *Cerebellum.* 16:203–229.
- Caligiore D, Pezzulo G, Miall RC, Baldassarre G. 2013. The contribution of brain sub-cortical loops in the expression and acquisition of action understanding abilities. *Neurosci Biobehav Rev.* 37:2504–2515.
- Callan DE, Terzibas C, Cassel DB, Callan A, Kawato M, Sato MA. 2013. Differential activation of brain regions involved with error-feedback and imitation based motor simulation when observing self and an expert's actions in pilots and non-pilots on a complex glider landing task. *Neuroimage.* 72:55–68.
- Calvo-Merino B, Grèzes J, Glaser DE, Passingham RE, Haggard P. 2006. Seeing or doing? Influence of visual and motor familiarity in action observation. *Curr Biol.* 16:1905–1910.
- Campbell MEJ, Mehrkanoon S, Cunnington R. 2018. Intentionally not imitating: Insula cortex engaged for top-down control of action mirroring. *Neuropsychologia.* 111:241–251.
- Caspers S, Zilles K, Laird AR, Eickhoff SB. 2010. ALE meta-analysis of action observation and imitation in the human brain. *Neuroimage.* 50:1148–1167.
- Cauda F, Costa T, Torta DM, Sacco K, D'Agata F, Duca S, Geminiani G, Fox PT, Vercelli A. 2012. Meta-analytic clustering of the insular cortex: characterizing the meta-analytic

- connectivity of the insula when involved in active tasks. *Neuroimage*. 62:343–355.
- Cavallo A, Ansuini C, Becchio C. 2015. The (un)coupling between action execution and observation: comment on “Grasping synergies: a motor-control approach to the mirror neuron mechanism” by D’Ausilio, Bartoli and Maffongelli. *Phys Life Rev*. 12:129–130.
- Cavanna AE, Trimble MR. 2006. The precuneus: a review of its functional anatomy and behavioural correlates. *Brain*. 129: 564–583.
- Cheney PD, Fetz EE. 1980. Functional classes of primate corticomotoneuronal cells and their relation to active force. *J Neurophysiol*. 44:773–791.
- Cheng K, Fujita H, Kanno I, Miura S, Tanaka K. 1995. Human cortical regions activated by wide-field visual motion: an H2 (15)O PET study. *J Neurophysiol*. 74:413–427.
- Christensen A, Giese MA, Sultan F, Mueller OM, Goerick SL, Ilg W, Timmann D. 2014. An intact action-perception coupling depends on the integrity of the cerebellum. *J Neurosci*. 34: 6707–6716.
- Cotterill RM. 2001. Cooperation of the basal ganglia, cerebellum, sensory cerebrum and hippocampus: possible implications for cognition, consciousness, intelligence and creativity. *Prog Neurobiol*. 64:1–33.
- Craig AD. 2003. Interoception: the sense of the physiological condition of the body. *Curr Opin Neurobiol*. 13:500–505.
- Cramer SC, Weisskoff RM, Schaechter JD, Nelles G, Foley M, Finklestein SP, Rosen BR. 2002. Motor cortex activation is related to force of squeezing. *Hum Brain Mapp*. 16: 197–205.
- Decety J, Grèzes J, Costes N, Perani D, Jeannerod M, Procyk E, Grassi F, Fazio F. 1997. Brain activity during observation of actions. Influence of action content and subject’s strategy. *Brain*. 120(Pt 10):1763–1777.
- Di Cesare G, Valente G, Di Dio C, Ruffaldi E, Bergamasco M, Goebel R, Rizzolatti G. 2016. Vitality forms processing in the insula during action observation: a multivoxel pattern analysis. *Front Hum Neurosci*. 10:267.
- Diedrichsen J. 2006. A spatially unbiased atlas template of the human cerebellum. *Neuroimage*. 33:127–138.
- Diedrichsen J, Balsters JH, Flavell J, Cussans E, Ramnani N. 2009. A probabilistic MR atlas of the human cerebellum. *Neuroimage*. 46:39–46.
- Diedrichsen J, White O, Newman D, Lally N. 2010. Use-dependent and error-based learning of motor behaviors. *J Neurosci*. 30:5159–5166.
- Diedrichsen J, Zotow E. 2015. Surface-based display of volume-averaged cerebellar imaging data. *PLoS One*. 10:e0133402.
- Dupont P, Orban GA, De Bruyn B, Verbruggen A, Mortelmans L. 1994. Many areas in the human brain respond to visual motion. *J Neurophysiol*. 72:1420–1424.
- D’Angelo E, Casali S. 2012. Seeking a unified framework for cerebellar function and dysfunction: from circuit operations to cognition. *Front Neural Circuits*. 6:116.
- D’Angelo E, Gandini Wheeler-Kingshott C. 2017. Modelling the brain: elementary components to explain ensemble functions. *Rivista Del Nuovo Cimento*. 40:36.
- E KH, Chen SH, Ho MH, Desmond JE. 2014. A meta-analysis of cerebellar contributions to higher cognition from PET and fMRI studies. *Hum Brain Mapp*. 35:593–615.
- Ebisch SJ, Perrucci MG, Ferretti A, Del Gratta C, Romani GL, Gallese V. 2008. The sense of touch: embodied simulation in a visuotactile mirroring mechanism for observed animate or inanimate touch. *J Cogn Neurosci*. 20:1611–1623.
- Ehrsson HH, Fagergren E, Forssberg H. 2001. Differential frontoparietal activation depending on force used in a precision grip task: an fMRI study. *J Neurophysiol*. 85:2613–2623.
- Evarts EV. 1968. Relation of pyramidal tract activity to force exerted during voluntary movement. *J Neurophysiol*. 31: 14–27.
- Fagg AH, Arbib MA. 1998. Modeling parietal-premotor interactions in primate control of grasping. *Neural Netw*. 11: 1277–1303.
- Filimon F, Nelson JD, Hagler DJ, Sereno MI. 2007. Human cortical representations for reaching: mirror neurons for execution, observation, and imagery. *Neuroimage*. 37:1315–1328.
- Flandin G, Friston KJ. 2017. Analysis of family-wise error rates in statistical parametric mapping using random field theory. *Hum Brain Mapp*.
- Friston K. 2012. Ten ironic rules for non-statistical reviewers. *Neuroimage*. 61:1300–1310.
- Friston KJ, Fletcher P, Josephs O, Holmes A, Rugg MD, Turner R. 1998. Event-related fMRI: characterizing differential responses. *Neuroimage*. 7:30–40.
- Friston KJ, Mechelli A, Turner R, Price CJ. 2000. Nonlinear responses in fMRI: the Balloon model, Volterra kernels, and other hemodynamics. *Neuroimage*. 12:466–477.
- Friston KJ, Williams S, Howard R, Frackowiak RS, Turner R. 1996. Movement-related effects in fMRI time-series. *Magn Reson Med*. 35:346–355.
- Garrison KA, Aziz-Zadeh L, Wong SW, Liew SL, Winstein CJ. 2013. Modulating the motor system by action observation after stroke. *Stroke*. 44:2247–2253.
- Gatti R, Rocca MA, Fumagalli S, Gattrysse E, Kerckhofs E, Falini A, Filippi M. 2017. The effect of action observation/execution on mirror neuron system recruitment: an fMRI study in healthy individuals. *Brain Imaging Behav*. 11:565–576.
- Gazzola V, Keysers C. 2009. The observation and execution of actions share motor and somatosensory voxels in all tested subjects: single-subject analyses of unsmoothed fMRI data. *Cereb Cortex*. 19:1239–1255.
- Glickstein M, Gerrits N, Kralj-Hans I, Mercier B, Stein J, Voogd J. 1994. Visual pontocerebellar projections in the macaque. *J Comp Neurol*. 349:51–72.
- Graybiel AM. 1998. The basal ganglia and chunking of action repertoires. *Neurobiol Learn Mem*. 70:119–136.
- Grèzes J, Decety J. 2001. Functional anatomy of execution, mental simulation, observation, and verb generation of actions: a meta-analysis. *Hum Brain Mapp*. 12:1–19.
- Hamilton AF, Grafton ST. 2008. Action outcomes are represented in human inferior frontoparietal cortex. *Cereb Cortex*. 18:1160–1168.
- Hermesdörfer J, Goldenberg G, Wachsmuth C, Conrad B, Ceballos-Baumann AO, Bartenstein P, Schwaiger M, Boecker H. 2001. Cortical correlates of gesture processing: clues to the cerebral mechanisms underlying apraxia during the imitation of meaningless gestures. *Neuroimage*. 14:149–161.
- Ishibashi R, Pobric G, Saito S, Lambon Ralph MA. 2016. The neural network for tool-related cognition: an activation likelihood estimation meta-analysis of 70 neuroimaging contrasts. *Cogn Neuropsychol*. 33:241–256.
- Ito M. 2008. Control of mental activities by internal models in the cerebellum. *Nat Rev Neurosci*. 9:304–313.
- Jovicich J, Peters RJ, Koch C, Braun J, Chang L, Ernst T. 2001. Brain areas specific for attentional load in a motion-tracking task. *J Cogn Neurosci*. 13:1048–1058.
- Kasess CH, Windischberger C, Cunnington R, Lanzenberger R, Pezawas L, Moser E. 2008. The suppressive influence of SMA

- on M1 in motor imagery revealed by fMRI and dynamic causal modeling. *Neuroimage*. 40:828–837.
- Keisker B, Hepp-Reymond MC, Blickenstorfer A, Meyer M, Kollias SS. 2009. Differential force scaling of fine-graded power grip force in the sensorimotor network. *Hum Brain Mapp*. 30:2453–2465.
- Kelly RM, Strick PL. 2003. Cerebellar loops with motor cortex and prefrontal cortex of a nonhuman primate. *J Neurosci*. 23:8432–8444.
- Kilner JM. 2011. More than one pathway to action understanding. *Trends Cogn Sci*. 15:352–357.
- Kilner JM, Friston KJ, Frith CD. 2007. Predictive coding: an account of the mirror neuron system. *Cogn Process*. 8: 159–166.
- Kim SG, Ogawa S. 2012. Biophysical and physiological origins of blood oxygenation level-dependent fMRI signals. *J Cereb Blood Flow Metab*. 32:1188–1206.
- Knauff M, Mulack T, Kassubek J, Salih HR, Greenlee MW. 2002. Spatial imagery in deductive reasoning: a functional MRI study. *Brain Res Cogn Brain Res*. 13:203–212.
- Koul A, Cavallo A, Cauda F, Costa T, Diano M, Pontil M, Becchio C. 2018. Action observation areas represent intentions from subtle kinematic features. *Cereb Cortex*. 28:2647–2654.
- Krekelberg B, Boynton GM, van Wezel RJ. 2006. Adaptation: from single cells to BOLD signals. *Trends Neurosci*. 29: 250–256.
- Kuhtz-Buschbeck JP, Ehrsson HH, Forssberg H. 2001. Human brain activity in the control of fine static precision grip forces: an fMRI study. *Eur J Neurosci*. 14:382–390.
- Kuhtz-Buschbeck JP, Gilster R, Wolff S, Ulmer S, Siebner H, Jansen O. 2008. Brain activity is similar during precision and power gripping with light force: an fMRI study. *Neuroimage*. 40:1469–1481.
- Leech R, Braga R, Sharp DJ. 2012. Echoes of the brain within the posterior cingulate cortex. *J Neurosci*. 32:215–222.
- Leung HC, Gore JC, Goldman-Rakic PS. 2002. Sustained mnemonic response in the human middle frontal gyrus during on-line storage of spatial memoranda. *J Cogn Neurosci*. 14: 659–671.
- Linás RR. 2009. Inferior olive oscillation as the temporal basis for motricity and oscillatory reset as the basis for motor error correction. *Neuroscience*. 162:797–804.
- Luks TL, Simpson GV. 2004. Preparatory deployment of attention to motion activates higher-order motion-processing brain regions. *Neuroimage*. 22:1515–1522.
- McGregor HR, Gribble PL. 2015. Changes in visual and sensory-motor resting-state functional connectivity support motor learning by observing. *J Neurophysiol*. 114:677–688.
- Mechelli A, Price CJ, Friston KJ. 2001. Nonlinear coupling between evoked rCBF and BOLD signals: a simulation study of hemodynamic responses. *Neuroimage*. 14:862–872.
- Menon V, Adelman NE, White CD, Glover GH, Reiss AL. 2001. Error-related brain activation during a Go/NoGo response inhibition task. *Hum Brain Mapp*. 12:131–143.
- Miall RC. 2003. Connecting mirror neurons and forward models. *Neuroreport*. 14:2135–2137.
- Molenberghs P, Cunnington R, Mattingley JB. 2012. Brain regions with mirror properties: a meta-analysis of 125 human fMRI studies. *Neurosci Biobehav Rev*. 36:341–349.
- Molenberghs P, Johnson H, Henry JD, Mattingley JB. 2016. Understanding the minds of others: a neuroimaging meta-analysis. *Neurosci Biobehav Rev*. 65:276–291.
- Morin O, Grèzes J. 2008. What is “mirror” in the premotor cortex? A review. *Neurophysiol Clin*. 38:189–195.
- Munzert J, Lorey B, Zentgraf K. 2009. Cognitive motor processes: the role of motor imagery in the study of motor representations. *Brain Res Rev*. 60:306–326.
- Naish KR, Houston-Price C, Bremner AJ, Holmes NP. 2014. Effects of action observation on corticospinal excitability: muscle specificity, direction, and timing of the mirror response. *Neuropsychologia*. 64:331–348.
- Nakata H, Sakamoto K, Ferretti A, Gianni Perrucci M, Del Gratta C, Kakigi R, Luca Romani G. 2008. Somato-motor inhibitory processing in humans: an event-related functional MRI study. *Neuroimage*. 39:1858–1866.
- Neely KA, Coombes SA, Planetta PJ, Vaillancourt DE. 2013. Segregated and overlapping neural circuits exist for the production of static and dynamic precision grip force. *Hum Brain Mapp*. 34:698–712.
- Oldfield RC. 1971. The assessment and analysis of handedness: the Edinburgh inventory. *Neuropsychologia*. 9:97–113.
- Palesi F, De Rinaldis A, Castellazzi G, Calamante F, Muhlert N, Chard D, Tournier JD, Magenes G, D’Angelo E, Gandini Wheeler-Kingshott CAM. 2017. Contralateral cortico-ponto-cerebellar pathways reconstruction in humans in vivo: implications for reciprocal cerebro-cerebellar structural connectivity in motor and non-motor areas. *Sci Rep*. 7:12841.
- Palesi F, Tournier JD, Calamante F, Muhlert N, Castellazzi G, Chard D, D’Angelo E, Wheeler-Kingshott CA. 2015. Contralateral cerebello-thalamo-cortical pathways with prominent involvement of associative areas in humans in vivo. *Brain Struct Funct*. 220:3369–3384.
- Pineda JA, Moore AR, Elfenbein H, Cox R. 2009. Hierarchically organized mirroring processes in social cognition: the functional neuroanatomy of empathy. In: Pineda JA, editor. *Mirror neuron systems: the role of mirroring processes in social cognition*. Totowa, NJ: Humana Press. p. 135–160.
- Porro CA, Facchin P, Fusi S, Dri G, Fadiga L. 2007. Enhancement of force after action observation: behavioural and neurophysiological studies. *Neuropsychologia*. 45:3114–3121.
- Ptak R. 2012. The frontoparietal attention network of the human brain: action, saliency, and a priority map of the environment. *Neuroscientist*. 18:502–515.
- Ramnani N. 2006. The primate cortico-cerebellar system: anatomy and function. *Nat Rev Neurosci*. 7:511–522.
- Reed CL, Shoham S, Halgren E. 2004. Neural substrates of tactile object recognition: an fMRI study. *Hum Brain Mapp*. 21: 236–246.
- Riehle A, MacKay WA, Requin J. 1994. Are extent and force independent movement parameters? Preparation and movement-related neuronal activity in the monkey cortex. *Exp Brain Res*. 99:56–74.
- Rizzolatti G, Craighero L. 2004. The mirror-neuron system. *Annu Rev Neurosci*. 27:169–192.
- Romaiguère P, Nazarian B, Roth M, Anton JL, Felician O. 2014. Lateral occipitotemporal cortex and action representation. *Neuropsychologia*. 56:167–177.
- Salama IM, Turner S, Edwards MG. 2011. Automatic priming of grip force following action observation. *Q J Exp Psychol (Hove)*. 64:833–838.
- Schmahmann JD. 1996. From movement to thought: anatomic substrates of the cerebellar contribution to cognitive processing. *Hum Brain Mapp*. 4:174–198.
- Schmahmann JD, Pandya DN. 1995. Prefrontal cortex projections to the basilar pons in rhesus monkey: implications for the cerebellar contribution to higher function. *Neurosci Lett*. 199:175–178.

- Schurz M, Radua J, Aichhorn M, Richlan F, Perner J. 2014. Fractionating theory of mind: a meta-analysis of functional brain imaging studies. *Neurosci Biobehav Rev.* 42:9–34.
- Sevdalis V, Keller PE. 2011. Captured by motion: dance, action understanding, and social cognition. *Brain Cogn.* 77:231–236.
- Shadmehr R, Mussa-Ivaldi S. 2012. *Biological learning and control.* Cambridge, MA: The MIT Press..
- Shima K, Tanji J. 1998. Both supplementary and presupplementary motor areas are crucial for the temporal organization of multiple movements. *J Neurophysiol.* 80:3247–3260.
- Shomstein S. 2012. Cognitive functions of the posterior parietal cortex: top-down and bottom-up attentional control. *Front Integr Neurosci.* 6:38.
- Smith AM, Hepp-Reymond MC, Wyss UR. 1975. Relation of activity in precentral cortical neurons to force and rate of force change during isometric contractions of finger muscles. *Exp Brain Res.* 23:315–332.
- Sokolov AA, Miall RC, Ivry RB. 2017. The cerebellum: adaptive prediction for movement and cognition. *Trends Cogn Sci.* 21:313–332.
- Spraker MB, Yu H, Corcos DM, Vaillancourt DE. 2007. Role of individual basal ganglia nuclei in force amplitude generation. *J Neurophysiol.* 98:821–834.
- Stefan K, Cohen LG, Duque J, Mazzocchio R, Celnik P, Sawaki L, Ungerleider L, Classen J. 2005. Formation of a motor memory by action observation. *J Neurosci.* 25:9339–9346.
- Stoodley CJ, Schmahmann JD. 2010. Evidence for topographic organization in the cerebellum of motor control versus cognitive and affective processing. *Cortex.* 46:831–844.
- Stoodley CJ, Valera EM, Schmahmann JD. 2012. Functional topography of the cerebellum for motor and cognitive tasks: an fMRI study. *Neuroimage.* 59:1560–1570.
- Strick PL, Dum RP, Fiez JA. 2009. Cerebellum and nonmotor function. *Annu Rev Neurosci.* 32:413–434.
- Tanaka S, Inui T, Iwaki S, Konishi J, Nakai T. 2001. Neural substrates involved in imitating finger configurations: an fMRI study. *Neuroreport.* 12:1171–1174.
- Thompson JC, Hardee JE, Panayiotou A, Crewther D, Puce A. 2007. Common and distinct brain activation to viewing dynamic sequences of face and hand movements. *Neuroimage.* 37:966–973.
- Thompson J, Parasuraman R. 2012. Attention, biological motion, and action recognition. *Neuroimage.* 59:4–13.
- Turella L, Pierno AC, Tubaldi F, Castiello U. 2009. Mirror neurons in humans: consisting or confounding evidence? *Brain Lang.* 108:10–21.
- Valchev N, Zijdwind I, Keyesers C, Gazzola V, Avenanti A, Maurits NM. 2015. Weight dependent modulation of motor resonance induced by weight estimation during observation of partially occluded lifting actions. *Neuropsychologia.* 66:237–245.
- Van Overwalle F, Baetens K. 2009. Understanding others' actions and goals by mirror and mentalizing systems: a meta-analysis. *Neuroimage.* 48:564–584.
- Van Overwalle F, Baetens K, Mariën P, Vandekerckhove M. 2014. Social cognition and the cerebellum: a meta-analysis of over 350 fMRI studies. *Neuroimage.* 86:554–572.
- Van Overwalle F, Baetens K, Mariën P, Vandekerckhove M. 2015. Cerebellar areas dedicated to social cognition? A comparison of meta-analytic and connectivity results. *Soc Neurosci.* 10:337–344.
- Van Overwalle F, D'aes T, Mariën P. 2015. Social cognition and the cerebellum: a meta-analytic connectivity analysis. *Hum Brain Mapp.* 36:5137–5154.
- Van Overwalle F, Mariën P. 2016. Functional connectivity between the cerebrum and cerebellum in social cognition: a multi-study analysis. *Neuroimage.* 124:248–255.
- Vanderwert RE, Fox NA, Ferrari PF. 2013. The mirror mechanism and mu rhythm in social development. *Neurosci Lett.* 540:15–20.
- Ward NS, Frackowiak RS. 2003. Age-related changes in the neural correlates of motor performance. *Brain.* 126:873–888.
- Wasson P, Prodoehl J, Coombes SA, Corcos DM, Vaillancourt DE. 2010. Predicting grip force amplitude involves circuits in the anterior basal ganglia. *Neuroimage.* 49:3230–3238.
- Watson TC, Becker N, Apps R, Jones MW. 2014. Back to front: cerebellar connections and interactions with the prefrontal cortex. *Front Syst Neurosci.* 8:4.
- Weaver J. 2015. Motor learning unfolds over different time-scales in distinct neural systems. *PLoS Biol.* 13:e1002313.
- Weigelt S, Muckli L, Kohler A. 2008. Functional magnetic resonance adaptation in visual neuroscience. *Rev Neurosci.* 19:363–380.
- Wiggett AJ, Downing PE. 2011. Representation of action in occipito-temporal cortex. *J Cogn Neurosci.* 23:1765–1780.
- Yamazaki T, Nagao S. 2012. A computational mechanism for unified gain and timing control in the cerebellum. *PLoS One.* 7:e33319.
- Yeo BT, Krienen FM, Sepulcre J, Sabuncu MR, Lashkari D, Hollinshead M, Roffman JL, Smoller JW, Zöllei L, Polimeni JR, et al. 2011. The organization of the human cerebral cortex estimated by intrinsic functional connectivity. *J Neurophysiol.* 106:1125–1165.